 CMC, vol.32, no.1, pp.61-79, 2012

Development of a Morphing Skin Based on the Honeycomb Reinforced Elastomer

C. Wang[1], J.H. Qiu[1,2], R. Nie[1], H.L. Ji[1] and W. Deng[1]

Abstract: The morphing skin has been a main obstacle in the real-world implementation of morphing aircrafts. This paper presents a morphing skin made of the elastomer reinforced by the honeycomb structure. A matrix made from elastomer provides possibilities to configure the morphing skin and the honeycomb structure with smaller in-plane modulus and larger out-of-plane modulus is thought to be suitable to reinforce the elastomer. The polyurethane elastomer is selected and synthesized by the casting method with the prepolymer approach, after which a tensile test is conducted to get its stress-strain relationship. To decrease the skin depth and diminish the local deformation in the honeycomb cell, the elastomer is filled into the honeycomb core rather than just working as the flexible face sheets, which leads to the so-called honeycomb reinforced elastomer. To present its mechanical properties finite element method is applied to analyze the morphing skin with a plug-in of commercial software Abaqus developed to model the skin in details. Different geometry and material parameters are taken into consideration with three kinds of results calculated namely, the equivalent tensile modulus, the non-dimensionalized equivalent three-point bending stiffness and the linear strain capacity. After the simulation analysis, samples of the morphing skins are fabricated by the compression molds method and the tensile tests have verified both the concept and the simulation results. At last, an optimization performed has shown a significant decline of the tensile modulus and out-of-plane displacement of the morphing skin.

Keywords: Morphing skin, Honeycomb, Elastomer, Simulation, Optimization

[1] State Key Laboratory of Mechanics and Control for Mechanical Structures, College of Aerospace Engineering, Nanjing University of Aeronautics and Astronautics, Nanjing, China

[2] Corresponding author: J.H Qiu, Address: College of Aerospace Engineering, Nanjing University of Aeronautics and Astronautics, Yudao Street 29, Nanjing 210016, China. Tel.: +86-25-84891123; fax: +86-25-84891123. *E-mail address*: qiu@nuaa.edu.cn.

1 Introduction

The morphing technology makes an aircraft have the ability to change its geometry parameters during flight [Jha and Kudva (2004)]. Since wings are the most influential parts of an aircraft, most of the designs are focused on the wings. The conventional fixed shape aircraft can only have the best performance in the established missions and can't adapt to the changed missions very well. Scientists and engineers have been interested in the field early from the Soviet Union telescoping wing demonstrator LIG-7 in the 1930s to the variable sweep wings appearing in the 1940s and becoming prevalent in the next two decades. In the Mission Adaptive Wing program (MAW) a smooth variable camber wing is installed onto the F-111 fighter making the demonstrator have the capability of changing the parameters of both the wing planform and wing airfoil [Gilbert (1981)]. A hingeless morphing leading and trailing edge with integral actuation mechanism based on the shape memory alloy is developed in the Smart Wing Project with comparisons to the trailing edge actuated by the conventional electric motors and piezoelectric motors [Kudva (2004)]. The unmanned morphing aircraft MFX-1 under a program called "Next Generation Morphing Structures (N-MAS)" is capable of large geometry changes including 200% in the aspect ratio, 70% in the wing area and 40% in the wing span [Bowman, Sanders, Cannon, Kudva, Joshi and Weisshaar (2007)]. For the researchers who want to make aircrafts perform more efficiently at different altitudes and speeds, the morphing technology has always been a great aspiration. Even though the previous programs have achieved success to some extent, there still remain many problems to be solved among which the morphing skin is a main obstacle.

In general three basic requirements of a morphing skin can be summarized below. Firstly, the morphing skin should have a sufficient strain capacity which means when the smart skin is deformed the skin material can't be broken. This can be described "be capable to morph". Secondly, the energy cost to actuate the skin to morph should be low enough which requires a low equivalent modulus in the morphing direction. This can be called "be easy to morph". Last but not least, the morphing skin should be able to carry the local aerodynamic loads and transmit the loads to the inner structure. The third requirement can be called "be safe to morph". To meet the requirements above, two basic approaches can be made. One is by change of material stiffness, such as the shape memory polymer, and the other is by stiffness tailoring. Aeroelastic tailoring is used to control aeroelastic deformation and affect the performance of the aircraft by embodying the directional stiffness into an aircraft structure [Shirk, Hertz and Weisshaar (1986)] and by the approach of stiffness tailoring different stiffness can be achieved in different directions, which is suitable for the design of morphing skins. Thill, Etches, Bond,

Potter and Weaver (2008; 2010) summarized the materials, structures and designs of morphing skins and made use of the composite corrugated structure in a morphing trailing edge, firstly by corrugated laminates and then by corrugated sandwich structures to overcome its drawback of the low out-of-plane stiffness. Gandhi and Anusonti-Inthra (2008) identified the desirable attributes of a flexible skin especially in the airfoil camber morphing and Olympio and Gandhi (2010a) presented the concept of the sandwich structure skin with a honeycomb core and two flexible face sheets. Bubert, Woods, Kothera and Wereley (2010) demonstrated a flexible matrix composites composed of elastomer and carbon fiber laminae which is supported by a flexible honeycomb made of durable plastics.

This article aims to present a morphing skin made of the elastomeric material and the directional reinforcement material, which is planned to be installed onto a morphing trailing edge mechanism. And the morphing skin is hoped to be stretched and compressed in one dimension with the max equivalent strain less than 5%. The following will describe first the conceptual development of the honeycomb reinforced elastomer, then the parametric study by numerical simulation in the finite element software Abaqus, together with the fabrication and the sample test. At last an optimization is performed to get better performance for a real-world implementation.

2 Conceptual development

Since the strain capacity is required, a matrix made from elastomer provides possibilities to configure the morphing skin. While a morphing skin purely made from elastomer material is too flexible to carry the aerodynamic loads, some kind of reinforcement material will be needed to stiffen the skin in the proper direction. The low stiffness in the morphing direction should be compensated by the high stiffness in the non-morphing direction to diminish the overall aerodynamic deformation, which means the morphing skin would be anisotropic. The honeycomb structure with relatively smaller in-plane modulus and larger out-of-plane modulus is thought to be suitable for the applications of the morphing skin. The in-plane sketch of a honeycomb cell can be described by the geometric parameters shown in Fig. 1, in which h is the vertical wall length, l is the inclined wall length, t is the honeycomb thickness and θ is the cell angle (counterclockwise rotation from x axis to the inclined wall represents positive value). The ratio of the thickness to the length t/l (the vertical wall has the same length to the inclined wall) is thought to represent the relative density of the structure. According to Gibson and Ashby's research (1997), the out-of-plane equivalent modulus is proportional to the honeycomb relative density and its in-plane equivalent modulus is proportional to the cube of it, both of which are influenced by the geometric parameters of the honey-

comb cell and the honeycomb material parameter, making the honeycomb structure have a larger out-of-plane modulus than the in-plane modulus.

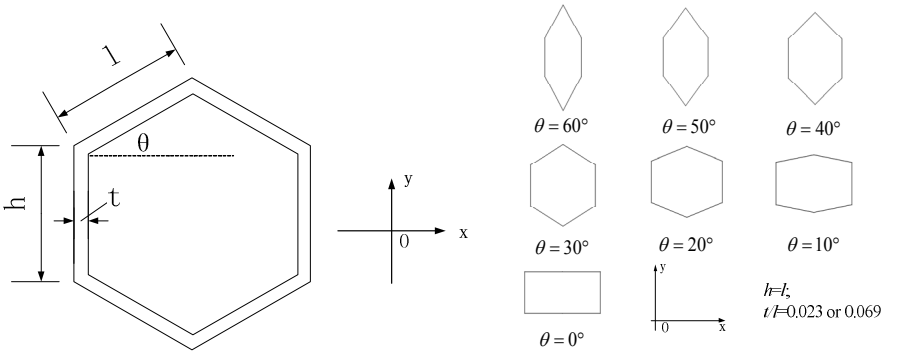

Figure 1: (a) The in-plane sketch of the honeycomb cell, (b) Cell shapes of the honeycomb

In the usual applications, the honeycomb is used as the core of the sandwich structure, carrying the shear load, stabilizing the face sheets [Mackerle (2002)]. While in the morphing skin proposed by Olympio and Gandhi (2010a) the modulus of the face sheet is quite low compared to those face sheets used in the ordinary honeycomb sandwich structures and the effects of the flexible face sheets on the bending stiffness can be neglected which is just needed to carry aerodynamic loads. As the side effect, the flexibility of face sheets will cause a larger depth of the morphing skin which means the increase of the weight and decrease of the inner space. The adhesion force between the core and the face sheets is small and aerodynamic loads may cause local deformations in the honeycomb cell especially as it has a considerable wall length.

A simple and direct method to make a good "trade-off" may be to fill the honeycomb core with the elastomer so the elastomer will be adhered to the honeycomb cell walls, thus the adhesion between the elastomer and the honeycomb will be enhanced substantially, eliminating the local deformation. Meanwhile, the elastomer filled in the honeycomb will increase the bending stiffness, which in turn will reduce the depth to get the same bending stiffness. In a viewpoint of manufacturing, a morphing skin based on the honeycomb core filled with elastomer could be easier to be fabricated compared to the morphing skin with the honeycomb core adhered to flexible face sheets, where the adhesive layer is necessary and might be broken under cyclic morphing. Thus, in this design the elastomer will be the flexible matrix and the honeycomb structure is used to reinforce it, which leads to

the so-called honeycomb reinforced elastomer. The flexible face sheets can also be added to make a sandwich structure, and different stiffening honeycombs can be used for different morphing aircrafts. Fig. 2 (a) shows the sketch of the honeycomb reinforced elastomer and Fig. 2 (b) describes the morphing skin composed of the flexible face sheet and the honeycomb reinforced elastomer. In this article, attention will be focused on the honeycomb reinforced elastomer.

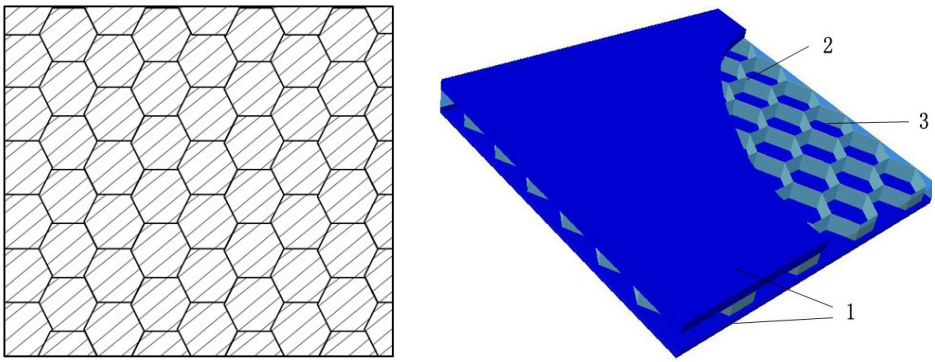

Figure 2: (a) Sketch of the honeycomb reinforced elastomer, (b) Morphing skin composed of the flexible face sheet and the honeycomb reinforced elastomer: 1: Flexible face sheets, 2: Honeycomb core, 3: Elastomer.

3 Numerical Simulation

3.1 Modeling of the honeycomb reinforced elastomer

To make the concept reality, some kind of elastomer with good mechanical and chemical properties is needed. The polyurethane (PU) is a kind of polymer and the polyurethane elastomer can be made in a variety of hardness, which makes it suitable for the attempt to develop the morphing skin.

There exist many ways to manufacture the PU elastomer namely, reaction injection molding, compression molding, casting into open molds and others. In the present study the casting method with the prepolymer is applied. The mechanical behavior of the elastomer is usually expressed in terms of strain energy potential based on two approaches: the physically-motivated model and the phenomenological model. The stress-strain relationship must be gained to simulate the mechanical response, thus a uniaxial tensile test according to the standard GB/T528-92 is conducted to test the elastomer sample. After the evaluation, the Yeoh model, a 3 order reduced

polynomial model, is selected to express the mechanical behavior of the elastomer. The nominal stress-strain relationship of the polyurethane elastomer is depicted in Fig. 3 from which one can conclude that PU elastomer has the hyperelastic property and in the medium morphing capacity focused by this article the elastomer can be seen as linear with a tangent modulus of about 8 MPa.

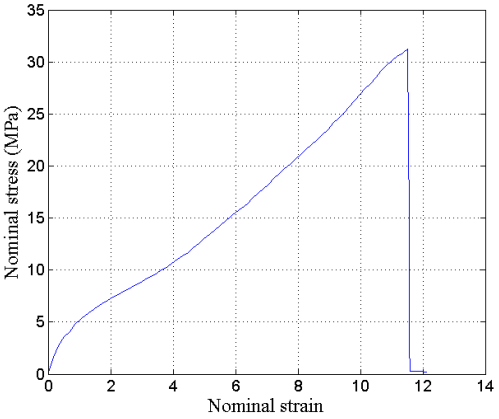

Figure 3: Nominal stress-strain relationship of the PU elastomer

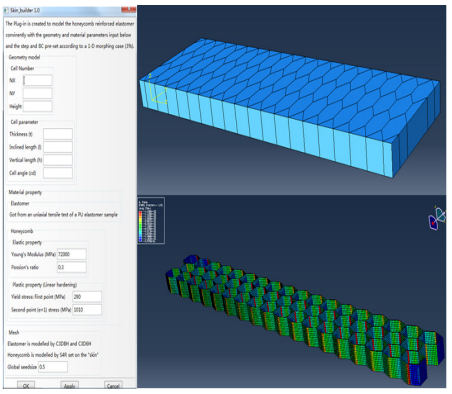

Figure 4: Plug-in interface and the finite element model

The honeycomb reinforced elastomer can be seen orthotropic whose constitutive law is written through the compliance matrix with the engineering constants: Young's Modulus: E_1, E_2, E_3, shear modulus: G_{12}, G_{13}, G_{23} and Poisson ratio: $\nu_{12}, \nu_{13}, \nu_{23}$ with the subscripts "1, 2, 3" pointing at x, y and z direction. Taking the nonlinear

properties of the elastomer into consideration, a more sophisticated expression can be written to express the stress-strain relationship with the superscript "*s*" added to represent the equivalent value in every small increment.

$$\begin{bmatrix} d\varepsilon_1 \\ d\varepsilon_2 \\ d\varepsilon_3 \\ d\varepsilon_4 \\ d\varepsilon_5 \\ d\varepsilon_6 \end{bmatrix} = \begin{bmatrix} \frac{1}{E_1^s} & -\frac{\upsilon_{12}^s}{E_2^s} & -\frac{\upsilon_{13}^s}{E_3^s} & 0 & 0 & 0 \\ -\frac{\upsilon_{21}^s}{E_1^s} & \frac{1}{E_2^s} & -\frac{\upsilon_{23}^s}{E_3^s} & 0 & 0 & 0 \\ -\frac{\upsilon_{31}^s}{E_1^s} & -\frac{\upsilon_{32}^s}{E_2^s} & \frac{1}{E_3^s} & 0 & 0 & 0 \\ 0 & 0 & 0 & \frac{1}{G_{23}^s} & 0 & 0 \\ 0 & 0 & 0 & 0 & \frac{1}{G_{31}^s} & 0 \\ 0 & 0 & 0 & 0 & 0 & \frac{1}{G_{12}^s} \end{bmatrix} \begin{bmatrix} d\sigma_1 \\ d\sigma_2 \\ d\sigma_3 \\ d\sigma_4 \\ d\sigma_5 \\ d\sigma_6 \end{bmatrix} \tag{1}$$

The morphing direction is defined in x direction. To evaluate the morphing skin, some parameters should be selected. The first is the strain capacity in the morphing direction, which can be found by determining the max stress in the morphing skin. The second is the equivalent modulus in the morphing direction. By seeing the morphing skin as a homogeneous material, the equivalent mechanical properties are calculated. The displacement loads are imposed at one end of the model while fixing the opposite. The imposed displacement represents the equivalent strain and the reaction forces at the imposed nodes are summarized to calculate the equivalent stress. And the value of equivalent tensile modulus is calculated by the expression below.

$$E_i = \frac{d\sigma_i}{d\varepsilon_i} = \frac{\sum (RF)_i / S}{\Delta L_i / L} \tag{2}$$

Here, $\sum (RF)_i$ is the reaction force, S and L are the area of the cross section and the length of the model respectively.

The third parameter is the equivalent bending stiffness B_i. The three-point bending test is usually applied to test the bending performance of a single plate. And to present the results more intuitively, the stiffness values are non-dimensionalized with respect to the 0.5 mm thick three-point bending-stiffness of the Al sheet skin with the same span and width to the morphing skin models. The three-point bending stiffness is calculated according to the expression below.

$$B_i = \frac{\Delta P}{\Delta f} = E_Y \frac{4bH^3}{S_l} \tag{3}$$

And, the components ΔP and Δf mean the increment of the load and the deflection. The components S_l, b and H represent the span, the width and depth of the model. The component E_Y represents the effect of material property. The honeycomb reinforced elastomer is modeled in details, and the similar computational approach

was presented by Chamis and Aiello (1988) to determine the equivalent mechanical and thermal properties of the metallic honeycomb core. The honeycomb and elastomer are modeled separately, then assembled and merged into one part with their original properties retained which indicates bonding between the honeycomb cell walls and the elastomer is thought to be perfect. The honeycomb structure is modeled by the shell element S4R and the hybrid elements C3D8H and C3D6H are used to model the elastomer. As to the material property, the honeycomb core material is idealized as bilinear [Papka and Kyriakides (1988)] and the elastomer material is thought to be hyperelastic, expressed by the Yeoh model selected. A plug-in based on Python language is developed for convenience and further study with which the finite element models generated can vary with input of the geometry and material parameters. Fig. 4 shows the plug-in interface and the finite element model generated.

Aluminum and polyoxymethylene (POM) are selected to reinforce the elastomer with the honeycomb material and geometry parameters summarized in Tab. 1. The volumetric relative density of the Al honeycomb core is determined based on a commercial Al honeycomb which the value of the POM honeycomb is set to be the same and triple to. As Fig. 1 (b) shows, 7 cell shapes are considered for every honeycomb parameter with the cell angle ranging from 0 to 60 degrees every 10 degrees. The height of the honeycomb is 5 mm for all the cell shapes.

Two load cases are necessary: the uniaxial tension and the three-point bending. The morphing skin models have 19 honeycomb cells in $x(y)$ direction and 3 cells in $y(x)$ direction which include about 50,000 to 100,000 elements in one model. Three kinds of results are calculated: the equivalent tensile modulus in x and y direction, the non-dimensionalized bending stiffness in x and y direction and the strain capacity in x direction.

Table 1: Honeycomb parameters

Honeycomb name	Young's Modulus (MPa)	Poisson Ratio	Yield Stress (MPa)	Ratio of the cell thickness to the cell length	Cell angle (degree)
Al-1	72000	0.3	145	0.023	Ranging from 0 to 60° every 10°
Al-2	72000	0.3	290	0.023	
POM-1	2600	0.4	63	0.023	
POM-2	2600	0.4	63	0.069	

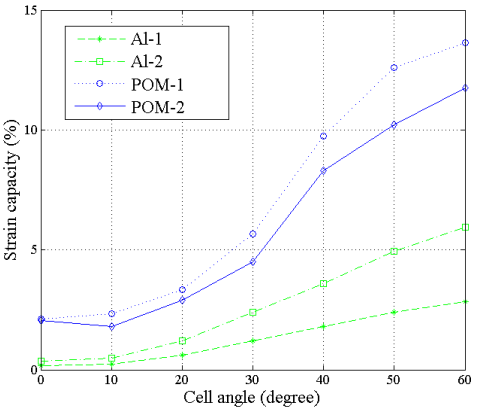

Figure 5: Linear strain capacity in x direction

3.2 Simulation Results

The linear strain capacity is calculated by determining whether the max stress of the morphing skin material has been beyond the yield stress, thus the honeycomb core material will be linearly elastic and elastomer material can also be thought to be linear since the capacity value is relatively much lower compared to the total strain capacity of elastomer gained from the test. As Fig. 5 shows the linear strain capacity will increase with the cell angle and a larger ratio of the yield stress to the Young's modulus of the honeycomb material will cause a larger linear strain capacity but the opposite results will be caused by the increase of the relative density of the honeycomb core.

As Fig. 6 and Fig. 7 show, the tensile modulus will be influenced by the cell angle and the honeycomb reinforced elastomer shows the anisotropic property. The larger tensile modulus in x (y) direction corresponds to the smaller one in y (x) direction. The regular hexagon honeycomb whose cell angle is 30 degrees is the critical instance where the tensile modulus in x and y directions are similar. Furthermore, comparing the modulus with different honeycomb parameters but the same cell angle, one can include that a larger honeycomb material Young's modulus and a larger relative density of the honeycomb core will lead to a larger equivalent modulus of the overall skin. Indeed, the equivalent tensile modulus can be as low as 10-20 MPa if proper geometry and material parameters are selected.

The relationships between the non-dimensionalized three-point bending stiffness and the cell angle are depicted in Fig. 8 and Fig. 9. While the trend is similar to the tensile modulus, what is important is the ability to carry aerodynamic loads. The

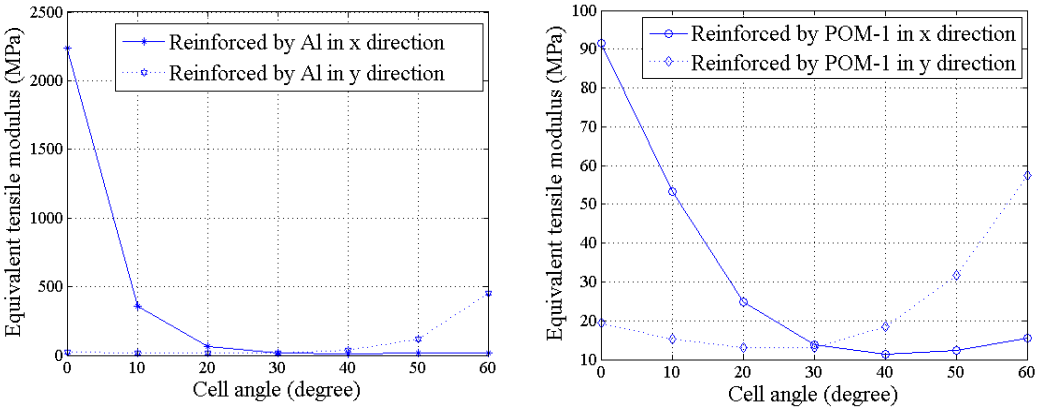

Figure 6: Equivalent tensile modulus of the elastomer reinforced by: (a) Al, (b) POM-1

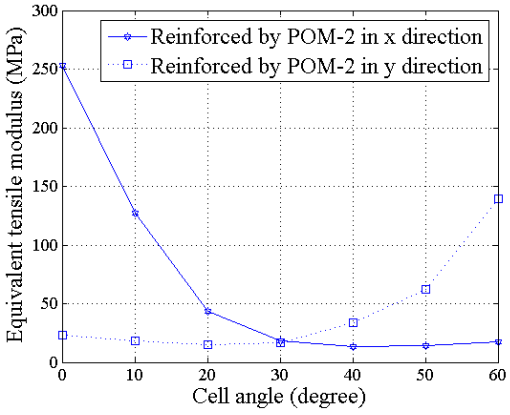

Figure 7: Equivalent tensile modulus of the elastomer reinforced by POM-2

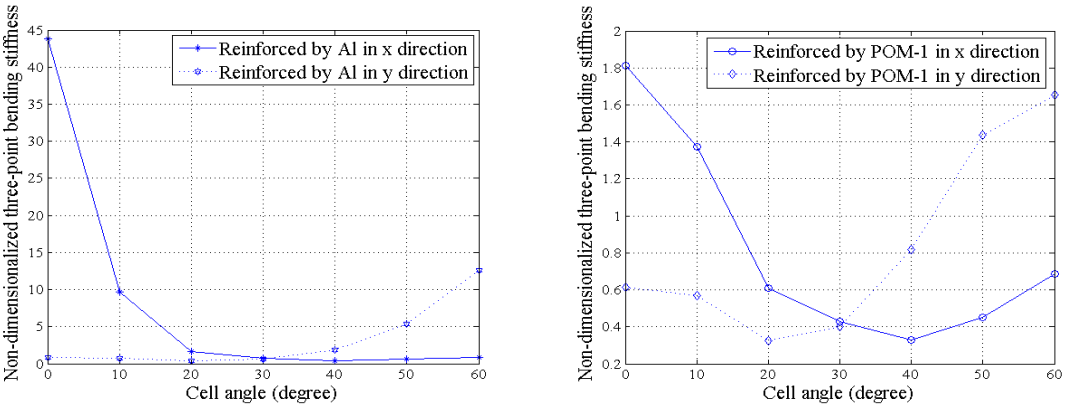

Figure 8: Non-dimensionalized three-point bending stiffness with: (a) Al, (b) POM-1 honeycomb

morphing skin models can reach 0.47 mm thick Al sheet model in x direction and 1.16 mm thick Al sheet model in y direction when the tensile modulus is as low as 10-20 MPa in x direction. The larger honeycomb material Young's modulus and relative density will come with the larger bending stiffness.

The results have indicated that by selecting the proper material and geometry properties the tensile modulus in the morphing direction can be reduced to a limited value with a much larger tensile modulus and bending stiffness in the other direction increasing the overall capability to carry aerodynamic loads. And a medium strain capacity requirement such as the morphing trailing edge can be satisfied with this skin concept.

4 Fabrication of the morphing skin and the sample test

After the simulation analysis, two kinds of samples are fabricated: one is the PU elastomer reinforced by the metallic regular hexagon honeycomb which has the same parameters to the simulation model Al-2, the other is reinforced by the POM honeycomb whose cell angle is 60 degrees. The POM honeycomb core is carved and cut by the laser thus the cell wall thickness is increased for convenience of manufacturing which leads to the increase of the cell wall length to keep the relative density unchanged. The skin samples are fabricated by the casting method and to control the depth of the elastomer the compression molds approach is applied as depicted in Fig. 10. The polytetrafluoroethylene (PTFE) film is used to prevent the bonding between the elastomer and molds. The elastomer is firstly casted into

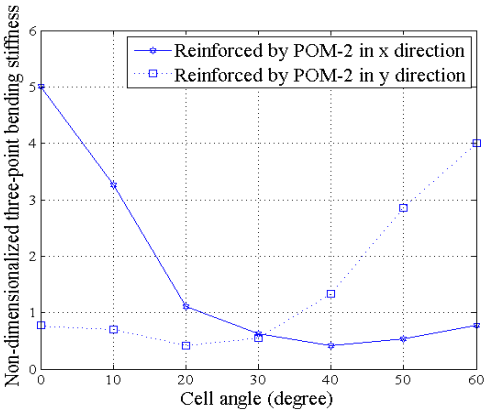

Figure 9: Non-dimensionalized three-point bending stiffness with POM-2 honeycomb

the molds from the spray gun before the honeycomb core is embedded, after which the solidification process will last about 5-7 days to provide the completed sample. The elastomer must be cured with the cell walls well to make the elastomer and the honeycomb core integrated as a whole part so the process of primer painting before the casting approach is added and the bonding is seen perfect in the simulation which may cause some errors to the real test.

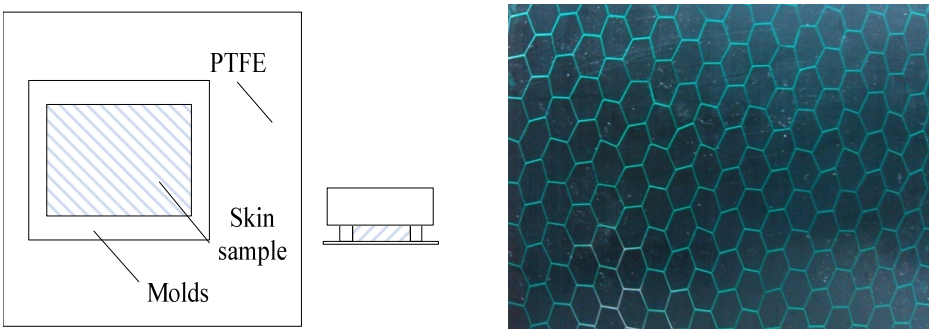

Figure 10: (a) Scheme of the compression molds, (b) Morphing skin sample

To verify the performance of the morphing skin, the uniaxial tensile test is made to attain the equivalent tensile modulus on the INSTRON 1185 testing machine as shown in Fig. 11. The samples are tailored for both the x and y direction ten-

sile test. Since no standards exist for the morphing skin test, the test condition is selected according to some similar standards. Tab. 2 summarizes the sample parameters and for the POM samples the ratio of the cell thickness to the cell length is not absolutely the same to the simulation model POM-2 because of the laser cauterization, thus their simulation results are re-calculated. The test results compared to the simulation results are summarized in Tab. 3, from which one can conclude there exist some errors between the finite element model and the real morphing skin sample that may be caused by the simulation process, the material properties input of which the elastomer properties may be influenced by the random of the handmade casting process. But in any case the tests have proved that the 30 degree instance is critical with the similar tensile modulus in x and y direction and the 60 degree instance will no doubt lead to an anisotropic property of the in-plane tensile modulus with one order of magnitude between x and y direction.

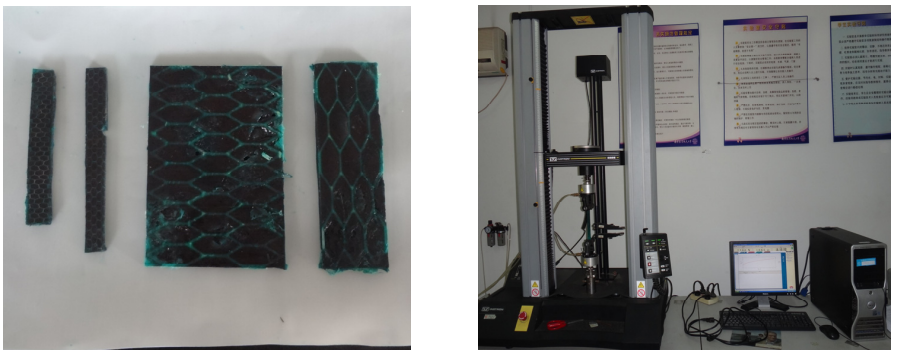

Figure 11: (a) Test samples, (b) Tensile test

Table 2: Morphing skin sample parameters

Sample name	Honeycomb material	Ratio of the cell thickness to the length (t/l)	Tensile direction
Sample-Al-x	Al	0.023	x
Sample-Al-y	Al	0.023	y
Sample-POM-x	POM	0.073	x
Sample-POM-y	POM	0.073	y

Table 3: Test results compared to the simulation

Sample name	Test result (MPa)	Simulation result (MPa)	Relative error
Sample-Al-x	19.14	20.22	5.64%
Sample-Al-y	15.58	17.48	12%
Sample-POM-x	18.33	17.75	3.16%
Sample-POM-y	172.58	145.99	15.41%

5 Optimization

The anisotropic property of the morphing skin has been verified by the parametric study and preliminary test in the above work. But for a real-world implementation, the morphing skins are required to be installed onto the morphing trailing edge as panels, which will lead all the skin boundaries to be fixed and (or) pinned, increasing the overall tensile modulus [Olympio and Gandhi (2010b)]. The contradictory requirements should be handled properly with proper parameters selected. Thus, the optimization procedure below is necessary to obtain better design parameters. An optimization was performed by Murugan, Saavedra Flores, Adhikari and Friswell (2012) to find the optimal fiber distribution for the fiber reinforced elastomer and the genetic algorithm was used to minimize the maximum out-of-plane displacement and maximize the in-plane displacement of the morphing skin panel.

To optimize the honeycomb reinforced elastomer, the finite element models are regenerated to provide morphing skins with 11 honeycomb cells in x and y direction each. Also two load cases are considered to calculate the equivalent tensile modulus E_1 and the maximum out-of-plane displacement U_{3ratio} caused by uniform loads and non-dimensionalized by the 0.5 mm thick Al sheet. The skin models are simply supported on the non-morphing sides and fixed on the other sides as depicted in Fig. 12.

Furthermore the small deflection w of an anisotropic thin plate can be derived from the following differential equation [Timoshenko and Woinowsky-Krieger (1959)]:

$$D_1\frac{\partial^4 w}{\partial x^4}+D_2\frac{\partial^4 w}{\partial y^4}+2D_3\frac{\partial^4 w}{\partial x^2\partial y^2}=q \tag{4}$$

In which:

$$D_1=\frac{E_1\delta^3}{12(1-\upsilon_{21}\upsilon_{12})}\quad D_2=\frac{E_2\delta^3}{12(1-\upsilon_{21}\upsilon_{12})}\quad D_3=\upsilon_{12}D_1+2D_k\quad D_k=\frac{G_{12}\delta^3}{12} \tag{5}$$

Here δ is the depth of the plate which is supposed to be a small value compared to the length and width of the plate and q is the loads imposed. Whereas the analytical expression of the deflection can only be obtained according to the boundary conditions which may sometimes lead to difficulties on mathematical derivation, it can be found that the deflection of the plate is influenced by the tensile modulus in both x and y direction, providing possibilities of designing a morphing skin with a low tensile modulus in the morphing direction but a relatively high bending stiffness to carry aerodynamic loads.

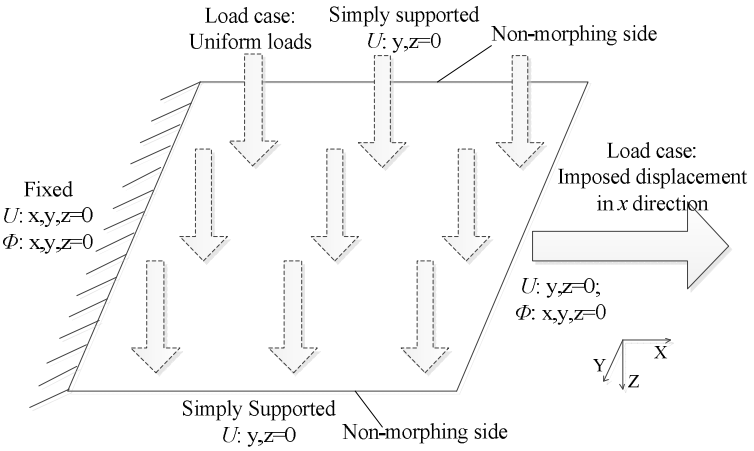

Figure 12: Boundary conditions and loads of the morphing skin model

The multi-discipline optimization software Isight is used to provide an optimization platform with Abaqus called and coupled by coding with Python language. The geometry parameters l, t, and θ of the honeycomb cell are selected to be design variables while the vertical length of the honeycomb h and the material parameters are kept unchanged as the POM case above. The optimization is required to minimize both the equivalent tensile modulus E_1 and the maximum non-dimensionalized displacement U_{3ratio}, introducing a multi-objective optimization problem which is preliminarily realized by the scalar method with each weight factor equal to 0.5 for instance. Moreover, the geometry constraint is included to prevent the honeycomb vertical and inclined walls from hitting each other. The variables, constraint and objective are summarized as follows:

Variables:

$$\begin{cases} l & 1.732 < l < 5.196\ (mm) \\ \theta & -90^\circ < \theta < 90^\circ \\ t & t \in \{0.04,\ 0.08,\ 0.12\}(mm) \end{cases} \tag{6}$$

Constraint:

$$h + 2l\sin\theta > 0 \tag{7}$$

Objective:

$$\min w_1 E_1 + w_2 U_{3ratio} \tag{8}$$

Here, w_i (i=1, 2) is the weight factor of each single objective. The multi-island genetic algorithm (MIGA) is a kind of distributed genetic algorithm whose population is divided into several smaller ones known as subpopulation in an island where the traditional genetic algorithm is performed separately. Information exchange among subpopulations is performed by moving some individuals from one subpopulation to another known as migration. Diversity can be preserved which may help to gain better optimization results by adopting the approach [Cantú-Paz (1998); Miki (1999)]. In this case, there are 10 generations and 5 islands with each subpopulation size equal to 10. The optimization process is described in Fig. 13.

The optimal results are summarized in Tab. 4 compared to the starting design point, showing the significant decline of the in-plane tensile modulus and the non-dimensionalized out-of-plane displacement. Further study can be done by changing the honeycomb geometry to a higher extent, making use of more proper material and applying a more suitable algorithm and agent model to get better results with less simulation time.

Table 4: Optimum design point compared to the starting one

Parameter name	l(mm)	t(mm)	θ (degree)	E_1(MPa)	U_{3ratio}
Starting design point	3.464	0.08	60.0	23.3	4.08
Optimum design point	4.746	0.04	45.521	18.92	2.73

6 Conclusions

In this paper to meet the diverse requirements the morphing skin based on the honeycomb reinforced elastomer is designed to be anisotropic with a low stiffness in

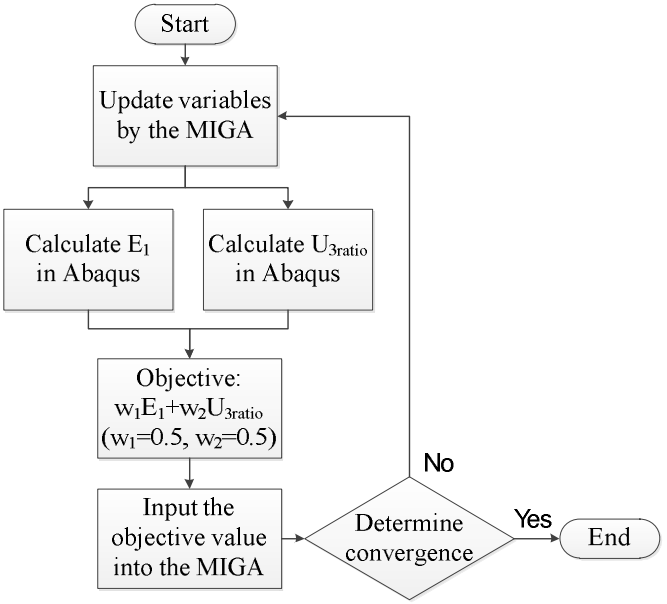

Figure 13: Optimization process of the morphing skin

the morphing direction and a high stiffness in the non-morphing direction. The equivalent mechanical properties of the morphing skin are influenced by the geometry parameters and material properties. The equivalent tensile modulus can be as low as 10-20 MPa in the morphing direction which can be one order of magnitude lower than that in the non-morphing direction and the equivalent bending stiffness has the similar trend that can reach the 0.5 mm to 1 mm thick Al sheet if proper parameters are selected. The linear strain capacity is also calculated in which the skin material can be seen linearly elastic, showing the adequate value for the morphing trailing edge application. Both the numerical simulation and the sample test have verified the honeycomb reinforced elastomer concept preliminarily. The optimization procedure is performed whose results have shown a significant performance improvement, which in turn indicates the application potential of the morphing skin. More attention can be devoted to better fabrication process and more proper optimization method with less calculation time, all of which is to make the morphing skin together with the morphing aircraft gradually become a real-world implementation.

Acknowledgement: The research is supported by the National Natural Science Foundation of China under Grant No.50830201, Program for Changjiang Scholars

and Innovative Research Team in University (PCSIRT) (NO.IRT0968), the Priority Academic Program Development of Jiangsu Higher Education Institutions and also supported by the Foundation of Graduate Innovation Center in NUAA (kfjj120102) and the Fundamental Research Funds for the Central Universities.

Reference

Bowman, J.; Sanders, B.; Cannon, B.; Kudva, J.; Joshi, S.; Weisshaar, T. (2007): Development of Next Generation Morphing Aircraft Structures. *Proceedings of 48th AIAA/ASME/ASCE/AHS/ASC Structures, Structural Dynamics, and Materials Conference.* United States.

Bubert, E.A.; Woods, B.; Kothera, C.; Wereley, N. (2010): Design and Fabrication of a Passive 1D Morphing Aircraft Skin. *Journal of Intelligent Material Systems and Structures*, vol. 21, pp. 1699-1717.

Cantú-Paz, E. (1998): A Survey on Parallel Genetic Algorithms. *Calculateurs Parallèles, Reseaux et Systems Repartis*, vol. 10, pp. 141–171.

Chamis, C.C.; Aiello, R.A.; Murthy, P.L.N. (1988): Fiber Composite Sandwich Thermostructural Behavior: Computational Simulation. *Journal of Composites Technology and Research*, vol. 10, pp. 93-9.

Gandhi, F.; Anusonti-Inthra, P. (2008): Skin Design Studies for Variable Camber Morphing Airfoils. *Smart Materials and Structures*, vol. 17, doi. 10.1088/0964-1726/17/01/015025.

Gibson, L.; Ashby, M. (1997): *Cellular Solids, Structures and Properties, 2nd edition.* Cambridge University Press.

Gilbert, W.W. (1981): Mission Adaptive Wing System for Tactical Aircraft. *Journal of Aircraft*, vol. 18, pp. 597-602.

Jha, A.K.; Kudva, J.N. (2004): Morphing Aircraft Concepts, Classifications, and Challenges. *Proceedings of SPIE Smart Structures and Materials: Industrial and Commercial Applications of Smart Structures Technologies*, vol. 5388, pp. 213-224.

Kudva, J.N. (2004): Overview of the DARPA Smart Wing Project. *Journal of Intelligent Material Systems and Structures*, vol. 15, pp. 261-267.

Mackerle, J. (2002): Finite Element Analyses of Sandwich Structures: A Bibliography (1980–2001). *Engineering Computations*, vol. 19, pp. 206-245.

Miki, M.; Hiroyasu, T.; Kaneko, M.; Hatanaka, K. (1999): A Parallel Genetic Algorithm with Distributed Environment Scheme. *Proceedings of IEEE International Conference on Systems, Man, and Cybernetics*, vol. 1, pp. 695-700.

Murugan, S.; Saavedra Flores, E.I.; Adhikari, S.; Friswell, M.I. (2012): Op-

timal Design of Variable Fiber Spacing Composites for Morphing Aircraft Skins. *Composite Structures*, vol. 94, pp. 1626-1633.

Olympio, K.R.; Gandhi, F. (2010a): Flexible Skins for Morphing Aircraft Using Cellular Honeycomb Cores. *Journal of Intelligent Material Systems and Structures*, vol. 21, pp. 1719-1735.

Olympio, K.R.; Gandhi, F. (2010b): Zero Poisson's Ratio Cellular Honeycomb for Flex Skins Undergoing One-Dimensional Morphing. *Journal of Intelligent Material Systems and Structures*, vol.21, pp. 1737-1753.

Papka, S.D.; Kyriakides, S. (1998): Experiments and Full-Scale Numerical Simulations of In-plane Crushing of a Honeycomb. *Acta Materialia*, vol. 46, pp. 2765-2776.

Shirk, M.H.; Hertz, T.J.; Weisshaar, T.A. (1986): Aeroelastic Tailoring—Theory, Practice, and Promise. *Journal of Aircraft*, vol. 23, pp. 6-18.

Thill, C.; Etches, J.; Bond, I.; Potter, K.; Weaver, P. (2008): Morphing Skins. *Aeronautical Journal*, vol. 112, pp. 117-139.

Thill, C.; Etches, J.A.; Bond, I.P.; Potter, K.D.; Weaver, P.M. (2010): Composite Corrugated Structures for Morphing Wing Skin Applications. *Smart Materials and Structures*, vol. 19, doi. 10.1088/0964-1726/19/12/124009.

Timoshenko, S.; Woinowsky-Krieger, S. (1959): *Theory of Plates and Shells, 2nd edition.* McGraw Hill Book Company.